R. & M. No. 3518

R. & M. No. 3518

MINISTRY OF TECHNOLOGY

AERONAUTICAL RESEARCH COUNCIL
REPORTS AND MEMORANDA

Exploratory Investigation of the Effects of Blowing from the Leading Edge of a Delta Wing

By W. J. G. Trebble, B.Sc.

LONDON: HER MAJESTY'S STATIONERY OFFICE
1968
PRICE 9s. 0d. NET

Exploratory Investigation of the Effects of Blowing from the Leading Edge of a Delta Wing

By W. J. G. Trebble, B.Sc.

Reports and Memoranda No. 3518*
April, 1966

Summary.
Low-speed wind-tunnel tests were made to investigate the possibility of increasing the lift of a highly swept wing by ejecting high energy air from the leading edge. The results showed that lift gains were available, but that care should be taken to direct the emergent jet with the minimum possible forward component so that large drag penalties may be avoided.

CONTENTS

*Replaces R.A.E. Tech. Report No. 66 125—A.R.C. 28 391.

1. *Introduction.*

The characteristic features of the flow over highly swept delta wings are produced by a pair of powerful vortices where spanwise location varies with sweepback and incidence[1]. These vortices give rise to large non-linear lift increments and from theoretical considerations Küchemann and Maskell suggested that additional lift may be available if the vortex strength could be artificially increased. With this end in view, they proposed that high energy air should be ejected from the leading edge.

The present Report discusses exploratory wind-tunnel tests made at the R.A.E. on a small model to investigate this proposal. From the lift point of view, the results were encouraging but, as the air was ejected normal to the leading edge, there was a large drag increment leading to a reduction in the lift/drag ratio. However, subsequently a more sophisticated model was made at the College of Aeronautics[2] which incorporated facilities for deflecting the emergent jet and thus reducing its dragwise component.

2. *Model Details.*

A model of a 70° swept delta wing with a 20 in. centreline chord was mounted inverted on a conventional wire rig from the overhead balance in the R.A.E. No. 1 4 ft × 3 ft wind-tunnel at Farnborough (Figs. 1 and 2). Originally it had been intended to provide a completely flat upper surface on the 0·8 in. thick slab wing but this was precluded by manufacturing difficulties. However, the flat area on the upper surface was kept as large as possible by offsetting the chordline 0·2 in. vertically. The leading edge was chamfered with a semi-angle of 16° measured normal to the leading edge, i.e. 5° along wind. The trailing-edge was bluff for the early tests, which included the flow visualisation but, in view of the large base-pressure drag ($C_p \approx -0{\cdot}4$), chamfer was applied to the trailing edge for the force measurements; this modification also gave a chamfer semi-angle of 16°.

Air was fed into the model through a simple air-bearing with three degrees of freedom (Fig. 2) mounted outside the tunnel though on the axis of rotation of the model. The air connection from the air-bearing to the model was generally constructed from circular pipes though a thick aerofoil section was achieved for that portion exposed to the tunnel air stream by the use of elliptic tubing with a wooden trailing-edge fairing. A suitable counter-balance weight arrangement was devised to reduce the pitching moment tare variation with incidence to an acceptable level (0·05 lb ft per degree).

Inside the model, the air was channelled along ten $\frac{1}{4}$ in. diameter ducts appropriately directed to feed two plenum chambers (Fig. 1) and was then ejected through narrow slots running along the wing leading edge. Unfortunately the difficulties of model construction again limited the design with the result that the blowing slot did not commence until $2\frac{1}{2}$ in. behind the apex. The slot geometry could be changed by altering adjustable screws spaced 0·6 in. apart along the slot and the following nozzle shapes were tested:

(A) Rectangular nozzle: width 0·006 in. throughout nozzle length.

(B) Tapered nozzle: width linearly increased from zero at front to 0·007 in. at back.

(C) Double tapered nozzle: width increased linearly from zero at front to 0·005 in. at two thirds length and then decreased linearly to zero at back.

(D) Polygonal nozzle: width increased linearly from zero at front to 0·005 in. at two thirds length then constant to back.

(E) Rear-end nozzle: nozzle closed to two thirds length then linearly increased to 0·010 in. at back.

As no attempt was made to direct the angle of ejection, the jets emerged normally to the leading edges. However, during subsequent tests by Alexander[2] on a larger model, thin grooved perspex strips were inserted in the slot thus producing a large number of small jets which could be deflected up to 80° backwards relative to the normal to the leading edge.

3. *Test Procedure.*

3.1. *Definitions and Measurement of Blowing Momentum Coefficient.*

The momentum coefficient $C\mu[\equiv mV_j/q_0\,Sg]$ is defined in terms of mass flow rate (m lb/sec) and the

theoretical jet velocity (V_J ft/sec), assuming isentropic expansion to free stream static pressure. In terms of the pressure ratio and mass flow rate:

$$C\mu = \frac{4{\cdot}572\, m\, T_D^{\frac{1}{2}}}{q_0 S}\left[1-(P_0/P_D)^{2/7}\right]^{\frac{1}{2}}$$

where P_0 and P_D are respectively the ambient pressure in the free stream and duct total pressure while T_D is the air total temperature in the duct.

The blowing system was calibrated at zero mainstream speed with the air-bearing sealed. The mass flow rate was measured with a 1·0 in. diameter orifice plate in a 3·0 in. diameter pipe and the temperature was obtained from a thermometer upstream of the air bearing. Total pressure (P_D lb/sq in.) was measured in each of the wing plenum chambers and hence a relationship was established between pressure ratio (P_0/P_D) and the blowing momentum. The majority of the tests were made at a mainstream speed of 120 ft/sec which gave a Reynolds number of $0{\cdot}84 \times 10^6$ based on the aerodynamic mean chord. However, a few measurements were also made at speeds of 50 ft/sec, 80 ft/sec and 150 ft/sec (Fig. 3) to check that the velocity of air ejection had no significant effect on the non-dimensional characteristics. At the standard mainstream speed of 120 ft/sec the pressure ratio was varied between 1·0 and 2·5 to give $C\mu$-values between 0 and 0·2.

3.2. *Corrections.*

Although normal wind-tunnel solid blockage corrections have been applied ($\Delta V/V = 0{\cdot}001$), no attempt has been made to correct for wake blockage which would be expected to be small in the absence of vortex breakdown. Conventional corrections were added for tunnel constraint:

$$\Delta\alpha = +0{\cdot}564\, C_L$$

$$\Delta C_D = +0{\cdot}0098\, C_L^2.$$

Corrections for the wire drag and resulting moment were calculated:

$$\Delta C_D\,(\text{tare}) = -0{\cdot}0246$$

$$\Delta C_m\,(\text{tare}) = -0{\cdot}0003\ (\alpha = 0); \quad +0{\cdot}0009\ (\alpha = 20°)$$

and the strut corrections were determined from measurements on the unblown model with and without the strut

$$\Delta C_D\,(\text{strut}) = -0{\cdot}0355\ (\alpha = 0); \quad -0{\cdot}0477\ (\alpha = 20°)$$

$$\Delta C_m\,(\text{strut}) = +0{\cdot}0192\ (\alpha = 0); \quad +0{\cdot}0194\ (\alpha = 10°).$$

The model was pivoted about a point 0·47 in. below the wing chord line at the fore and aft position of the mean quarter-chord point. Subsequently the moments were converted to values about the chordline height at the mean quarter-chord point.

4. *Results and Discussion.*

4.1. *Flow Visualisation.*

Surface flow studies on the unblown wing (Fig. 4) revealed the typical patterns produced by vortex flow over a delta wing with secondary separation lines at about 80 per cent of the semi-span. The application of blowing through the tapered nozzle moved the secondary separation lines outboard and, at a $C\mu$-value of 0·2, the separation had moved so close to the leading edge that the secondary flow patterns

had virtually disappeared. Unfortunately, for structural reasons the blowing slot did not commence until 2·5 in. behind the apex so the complex flow ahead of this point persisted even when blowing was applied. Comparison of Figs. 4a and b showed little difference in the general flow behaviour at C_L-values of 0·2 and 0·8 except that, as expected, the flow attachment lines on the upper surface lay further inboard at the higher lift when the vortex strength was greater.

At a C_L-value of 0·6, the vortex flow above the wing was studied by making a wake survey in a vertical plane containing the wing trailing edge (Fig. 5). This survey was limited to measurements of the total head with Kiel-tubes as, at the time of the tests, a suitably sized 5-tube head[4] did not exist for the 4 ft × 3 ft tunnel although one has since been provided. Fortunately, other work[5] had shown that the minimum pressure occurred at the vortex core which could thus be located. On the unblown wing the core was at 70 per cent semi-span but moved out as the blowing momentum was increased thus confirming the deductions from the surface flow studies. Simultaneously with this outward movement, the core size increased but there was insignificant change in the magnitude of the lowest measured pressure as the blowing momentum increased. However, some regions of pressure greater than mainstream total head were observed around the outside of the core; these were the remnants of the high energy emergent jet.

4.2. *Balance Measurements.*

Typical curves of the variation of lift increment with blowing momentum are shown in Fig. 6 for the tapered slot configuration. At low incidence, the lift gains were less than the applied blowing momentum but significant benefits were available at incidences above 8°. As the blowing momentum was increased, the rate of increase in lift was reduced and, at the higher incidences, a maximum lift increment was obtained at a $C\mu$-value rather less than 0·2. Consideration of all the results suggests that the maximum gains were achieved at an incidence of about 12° with lift increments up to half as much again as the applied blowing momentum. Alexander[3] was later able to demonstrate that some further lift benefits could be obtained by downward deflection of the jets.

Fig. 7a to e gives the lift and pitching moment results for blowing from the various nozzles with a range of $C\mu$-values from 0 to 0·2 and the relative effectiveness of the different nozzles is compared at $C\mu$-values of 0·025 and 0·10 in Fig. 8a and b. Although the rear-end slot (E) proved to be the most effective with the smaller blowing momentum, the taper slot was superior at the higher values of blowing momentum. This latter result was anticipated since a tapered nozzle would give rise to a momentum distribution appropriate to a conical flow field. Nozzles with a relatively large area ahead of the centre of gravity (e.g. the double tapered slot C) gave nose-up moment increments, while nozzles with a large area aft of the centre of gravity (e.g. the rear-end slot E) gave nose-down moment contributions. The tapered slot (B) also produced some nose-down moment contribution but this would be expected from an alleviation of the trailing-edge effect and consequent improvement in the loading over the rear part of the wing.

Before considering the drag results, care must be taken to ensure correct definitions of aircraft drag and engine thrust which must be equal in magnitude for trimmed level flight. The longitudinal force (F) measured on the balance should thus be increased by the blowing momentum (μ) to give the total drag (D). Taking this into account, the lift/drag ratios and also the lift/longitudinal force ratios have been plotted against lift in Fig. 9a to e and comparisons at $C\mu$-values of 0·025 and 0·10 are shown in Fig. 10. At all C_L-values there was a considerable reduction in the lift/drag ratio as the blowing momentum was increased though, at the higher C_L-values, gains were apparent if merely the C_L/C_F-values were considered. It was considered reasonable to expect that improvements in the lift/drag ratio would have accrued if the blowing momentum had been directed with a smaller forward component. Thus, a comparison is given between Figs. 11 and 12 of the actual measured drag for the tapered slot configuration and the calculated drag with the forward component of momentum removed assuming that this would result in no consequential changes in the lift values. Quite significant drag reductions due to blowing then seemed possible at C_L-values above 0·5. This line of investigation was later pursued by Alexander[2,3], who successfully deflected the emergent air 80° rearwards in the chordal plane with little deterioration of the lift gains at low $C\mu$-values.

5. *Concluding Remarks.*

These exploratory tests confirmed that lift gains were obtainable by ejecting high energy air from the leading edge of a delta wing. The optimum nozzle shape proved to be a tapered slot which would be expected to give the momentum distribution appropriate to conical flow. The lifting efficiency varied with incidence with the largest gains occurring at about 12°; i.e. a realistic landing attitude. As the air was ejected normally to the leading edge, a large drag penalty was incurred. Subsequent tests at the College of Aeronautics (Cranfield) have suggested that this could be reduced substantially by appropriately directing the angle of the emergent jet, without an appreciable fall-off in lifting efficiency. Further studies towards optimising such blowing configurations and providing a more reliable basis for lift/drag analysis are needed if realistic project studies are required.

LIST OF SYMBOLS

S	Wing area
c_0	Centreline chord
$\bar{c}$	Aerodynamic mean chord $= 2\,c_0/3$
ϕ	Leading-edge sweepback angle
α	Angle of incidence
T_D	Total temperature in duct
P_D	Total pressure in duct
P_o	Ambient pressure
q_0	Mainstream dynamic head
μ	Blowing momentum
C_L	Lift coefficient $=$ lift$/q_0\,S$
C_D	Drag coefficient $=$ drag$/q_0\,S$
C_m	Pitching-moment coefficient $=$ moment$/q_0\,S\,\bar{c}$
$C\mu$	Blowing-momentum coefficient $= \mu/q_0\,S$

REFERENCES

No.	*Author(s)*	*Title, etc.*
1	P. B. Earnshaw and J. A. Lawford	Low-speed wind tunnel experiments on a series of sharp-edged delta wings. Part II. Surface flow patterns and boundary layer transition measurements. A.R.C. R. & M. 3424. March 1964.
2	A. J. Alexander	Experiments on a delta wing using leading-edge blowing to remove the secondary separation. A.R.C. 24996. May 1963.
3	A. J. Alexander	Experimental investigation on a cropped delta with edge blowing. A.R.C. 25213. June 1963.
4	A. Spence and W. J. G. Trebble	Low-speed tunnel tests on the flow structure behind a body of revolution of fineness ratio $16\frac{2}{3}$: 1. R.A.E. Technical Note Aero 2406. A.R.C. 18562. October 1955.
5	D. A. Kirby	Low-speed wind-tunnel tests on a fully tapered wing with 81° leading edge sweep and a 6 per cent thick R.A.E. 101 section. R.A.E. Tech. Memo. Aero 449. A.R.C. 18139. November 1955.

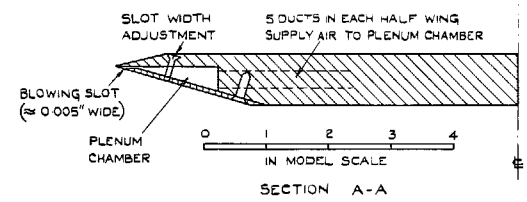

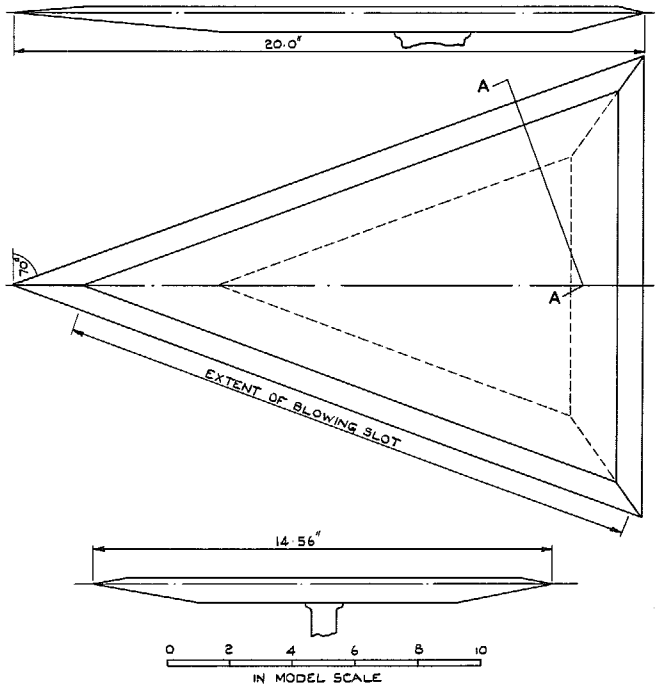

FIG. I G.A. OF DELTA WING

FIG. 1. G.A. of delta wing.

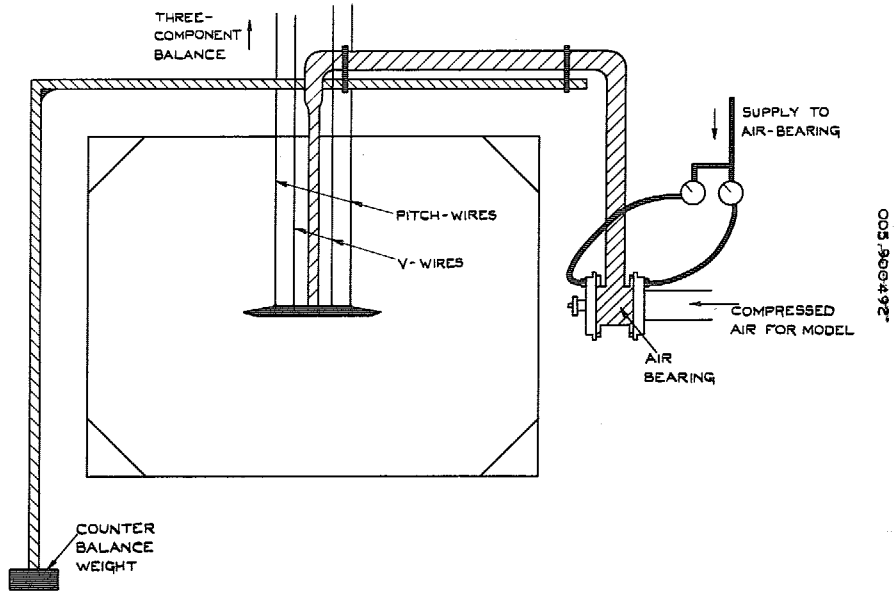

FIG. 2. Schematic view of model in 4 ft × 3 ft tunnel.

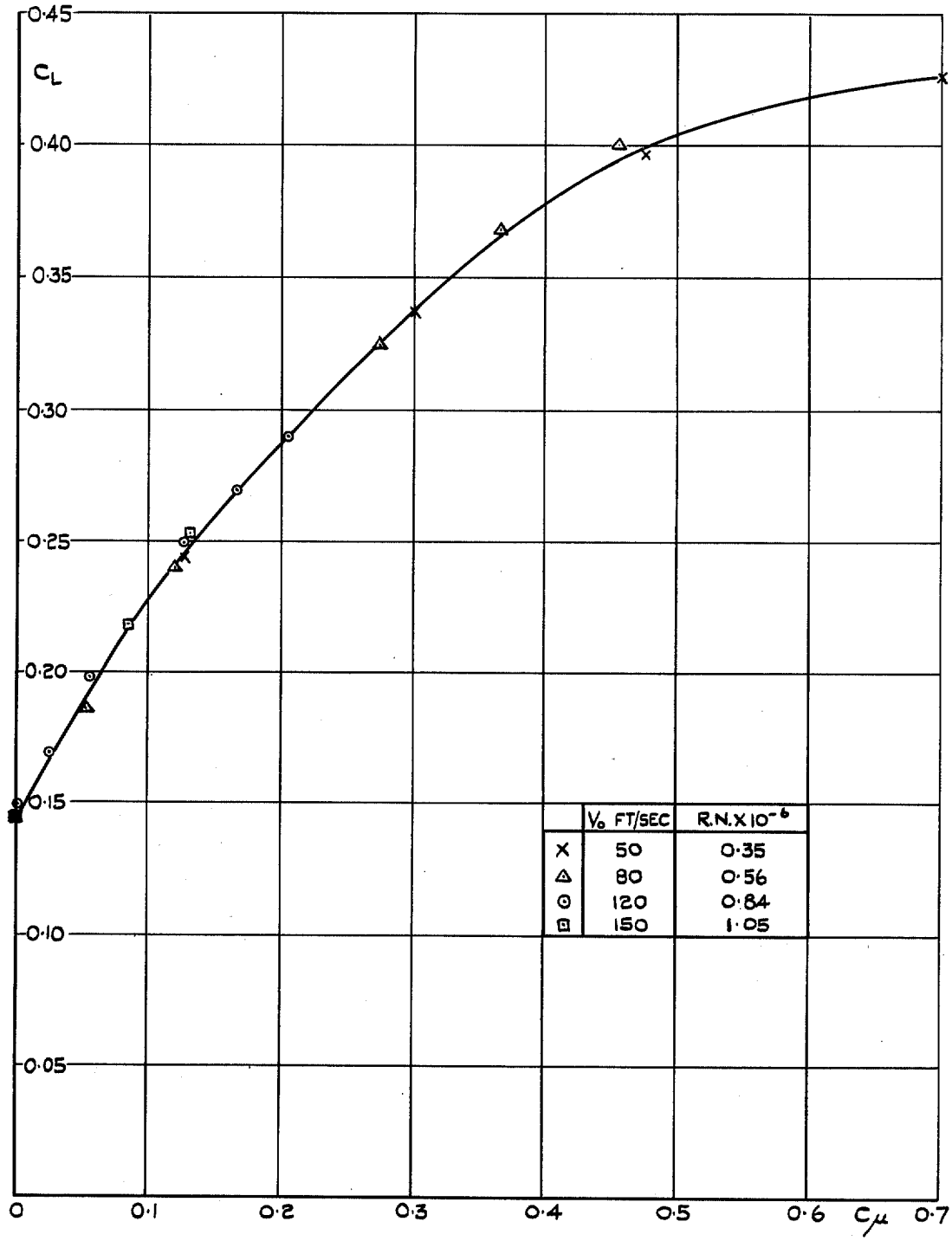

FIG. 3. Effect of Reynolds number on lift, $\alpha = 4{\cdot}2°$.

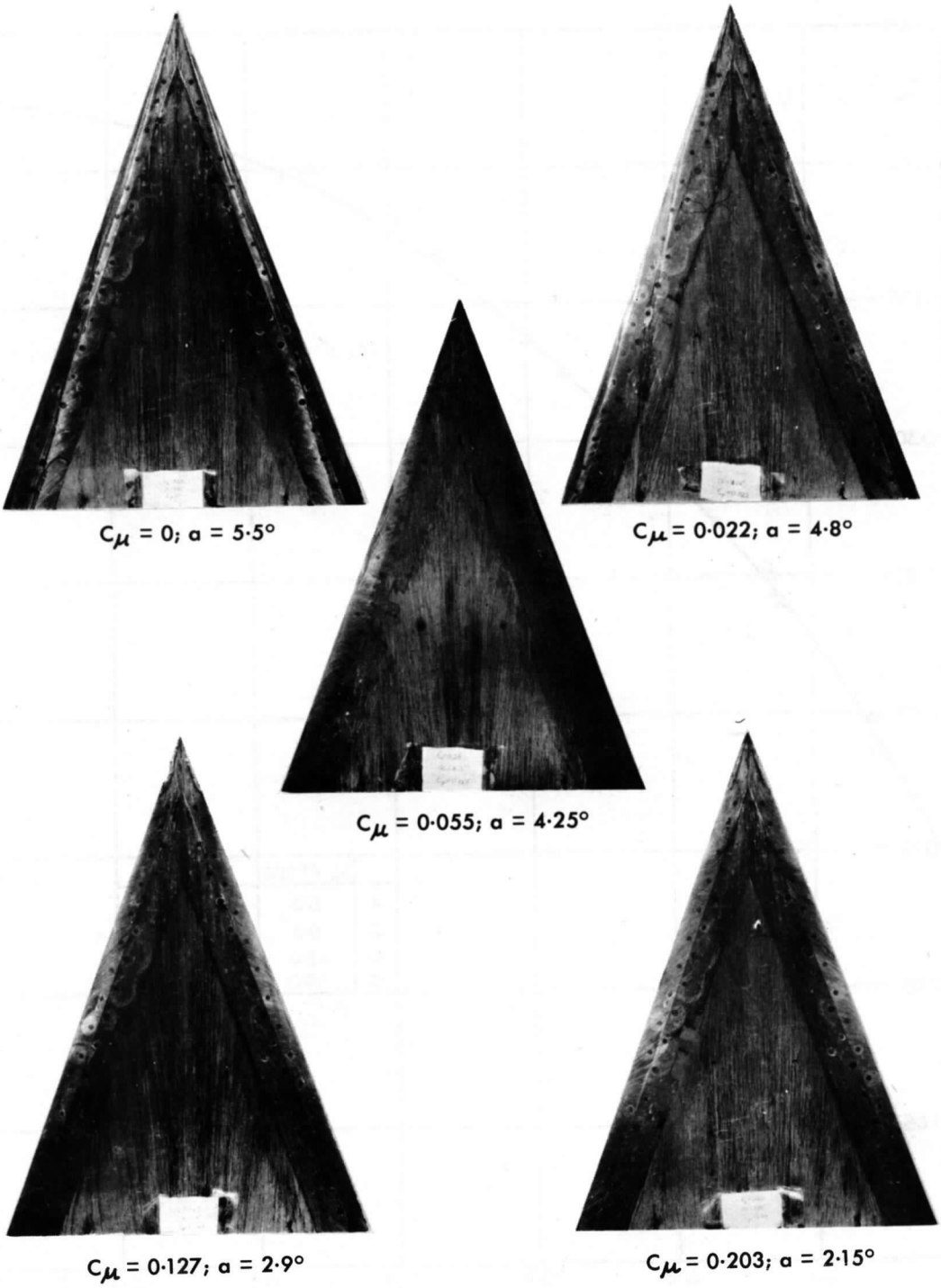

FIG. 4a. Surface flow patterns (a) $C_L = 0{\cdot}2$.

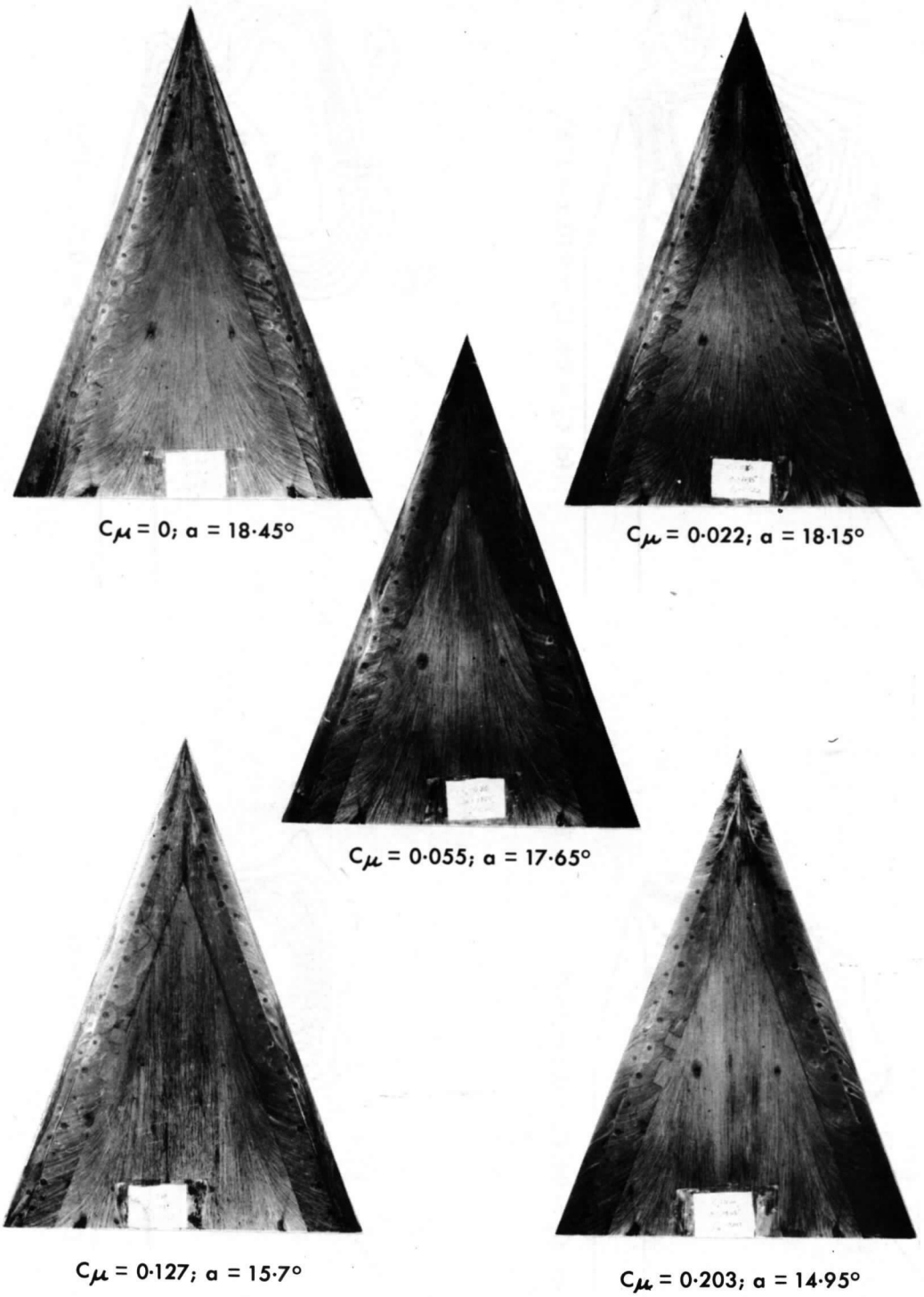

FIG. 4b. Surface flow patterns (b) $C_L = 0{\cdot}8$.

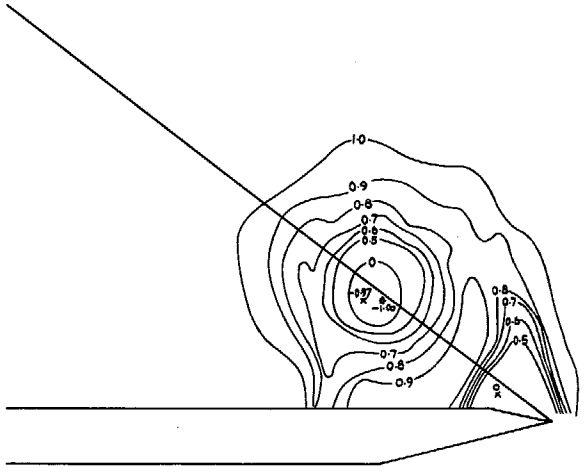

(a) $C_L = 0{\cdot}6, C_\mu = 0, \alpha = 16{\cdot}2°$.

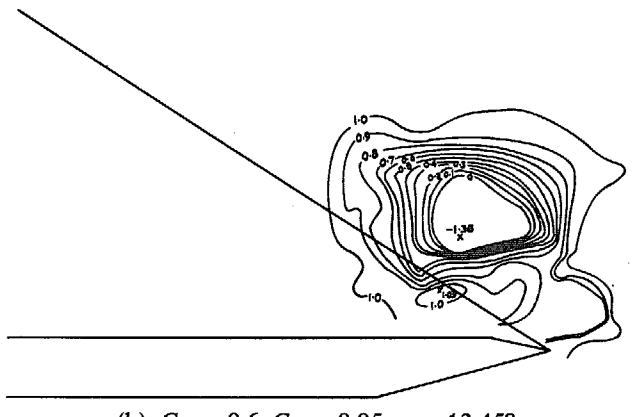

(b) $C_L = 0{\cdot}6, C_\mu = 0{\cdot}05, \alpha = 13{\cdot}45°$.

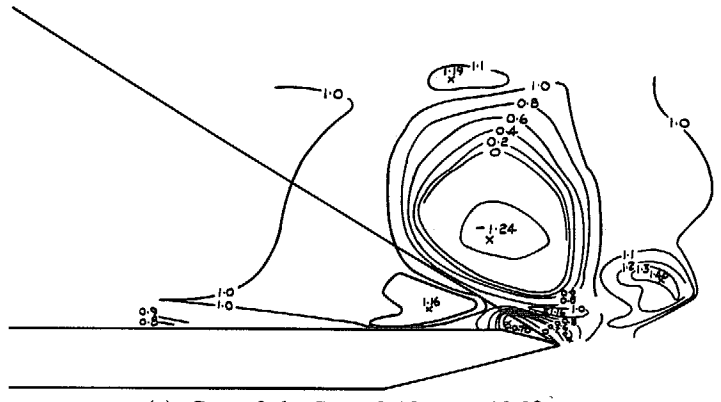

(c) $C_L = 0{\cdot}6,\ C_\mu = 0{\cdot}10, \alpha = 12{\cdot}8°$.

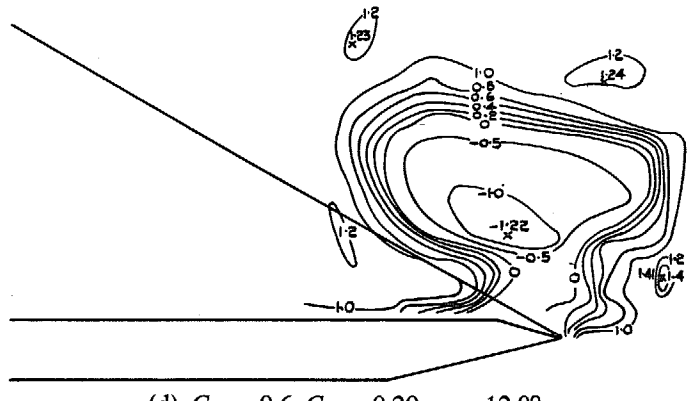

(d) $C_L = 0{\cdot}6, C_\mu = 0{\cdot}20, \alpha = 12{\cdot}0°$.

FIGS 5a to d. Total head pressure distribution at plane through trailing edge.

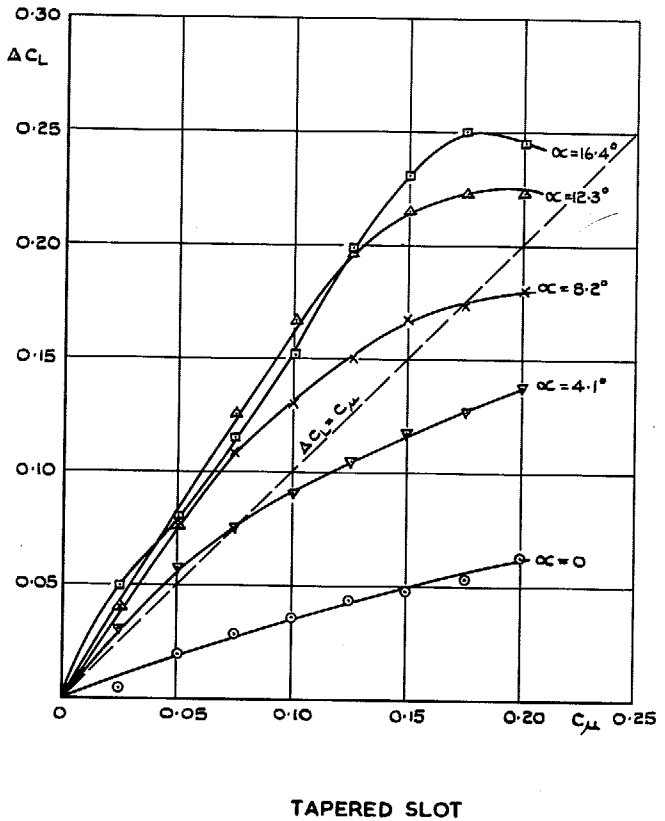

FIG. 6. Effect of momentum coefficient on lift increment.

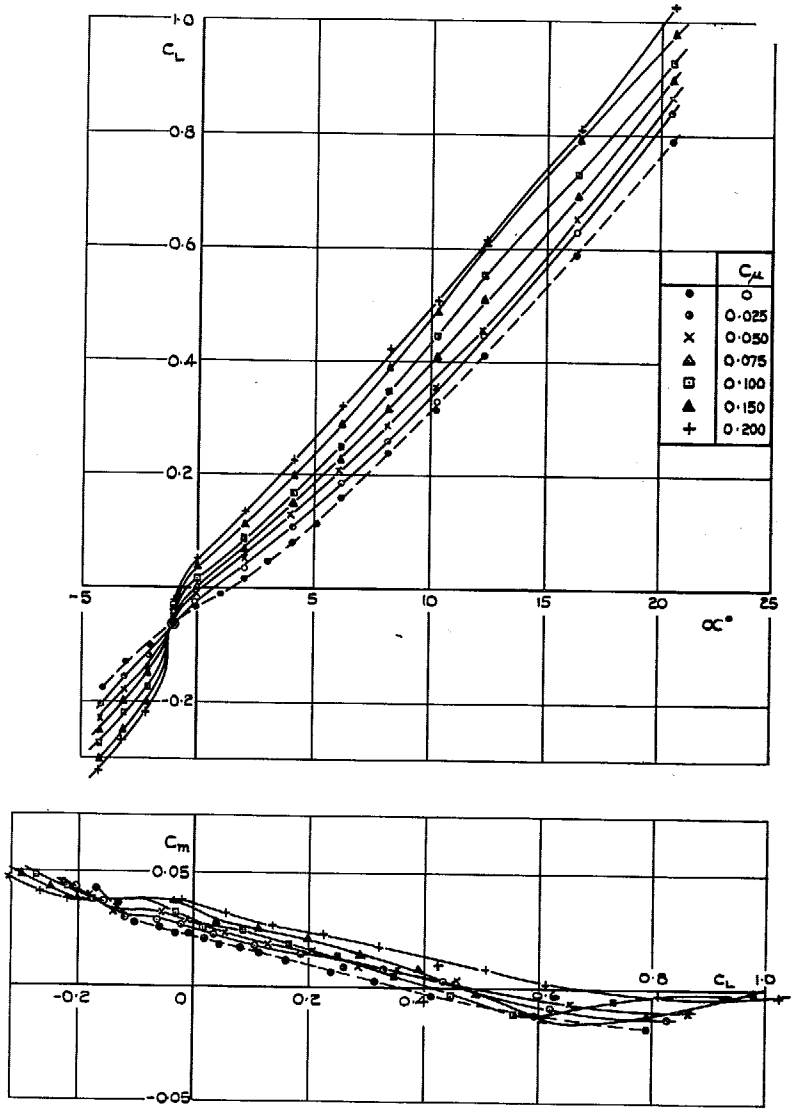

FIG. 7a. Lift and pitching moment. Rectangular slot 'A'.

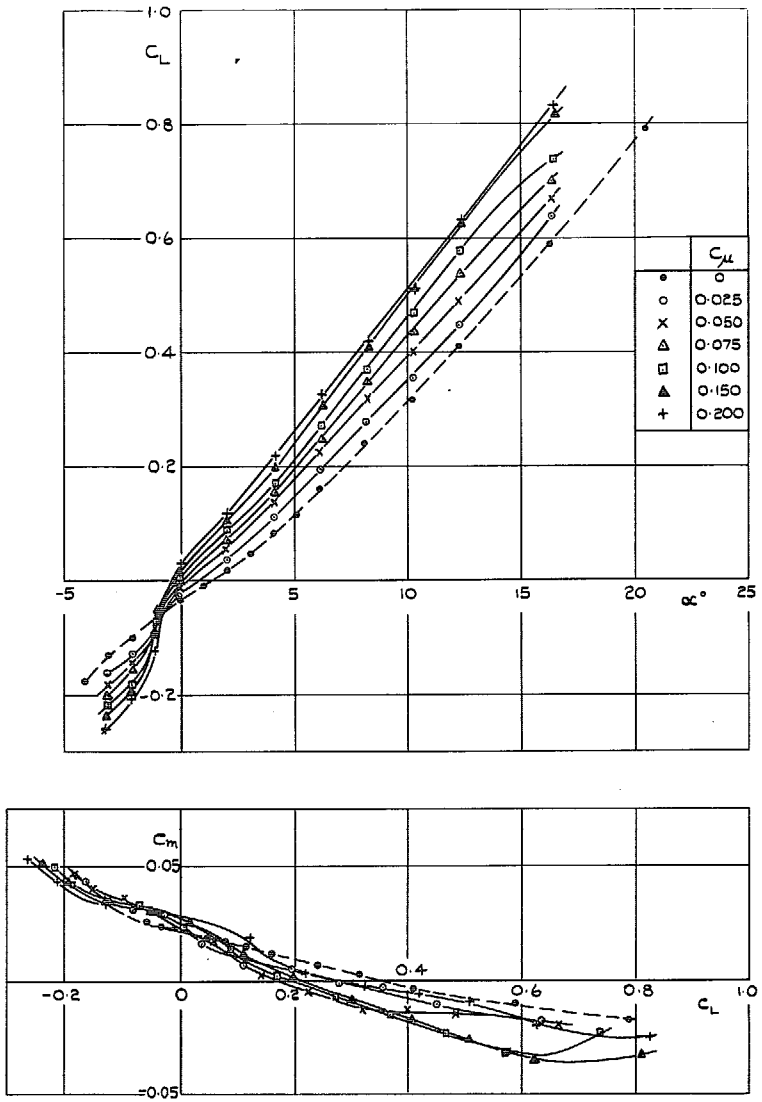

FIG. 7b. Lift and pitching moment. Tapered slot 'B'.

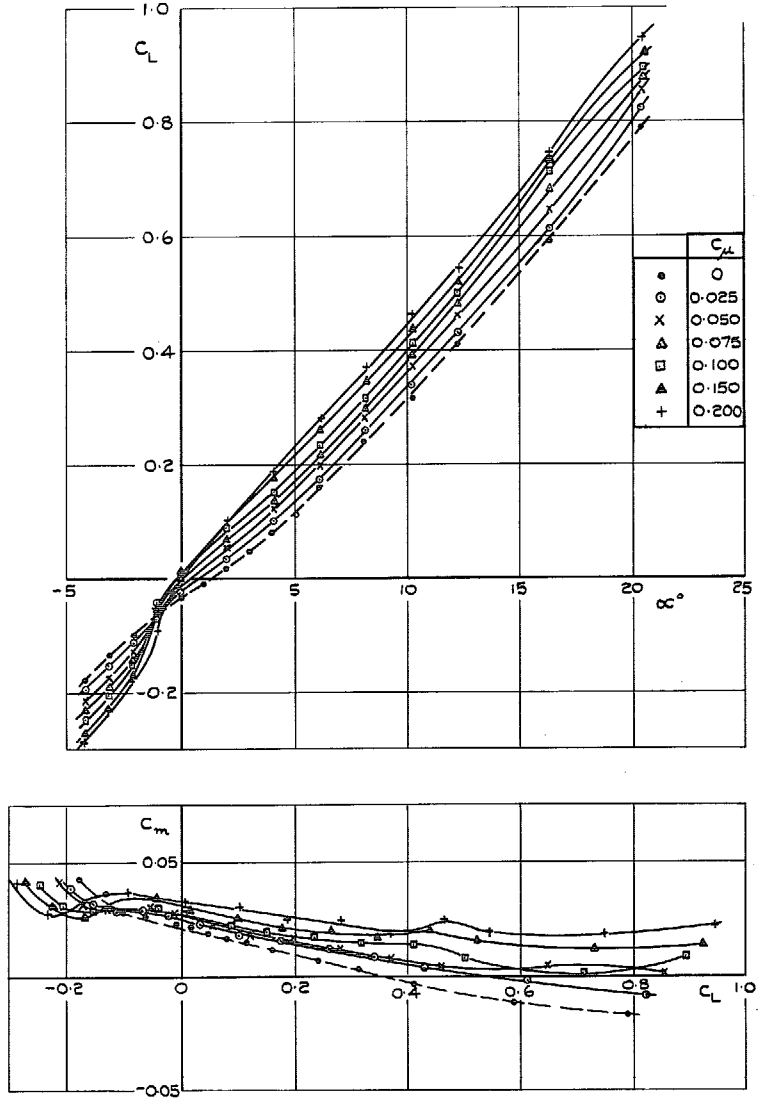

FIG. 7c. Lift and pitching moment. Double tapered slot 'C'.

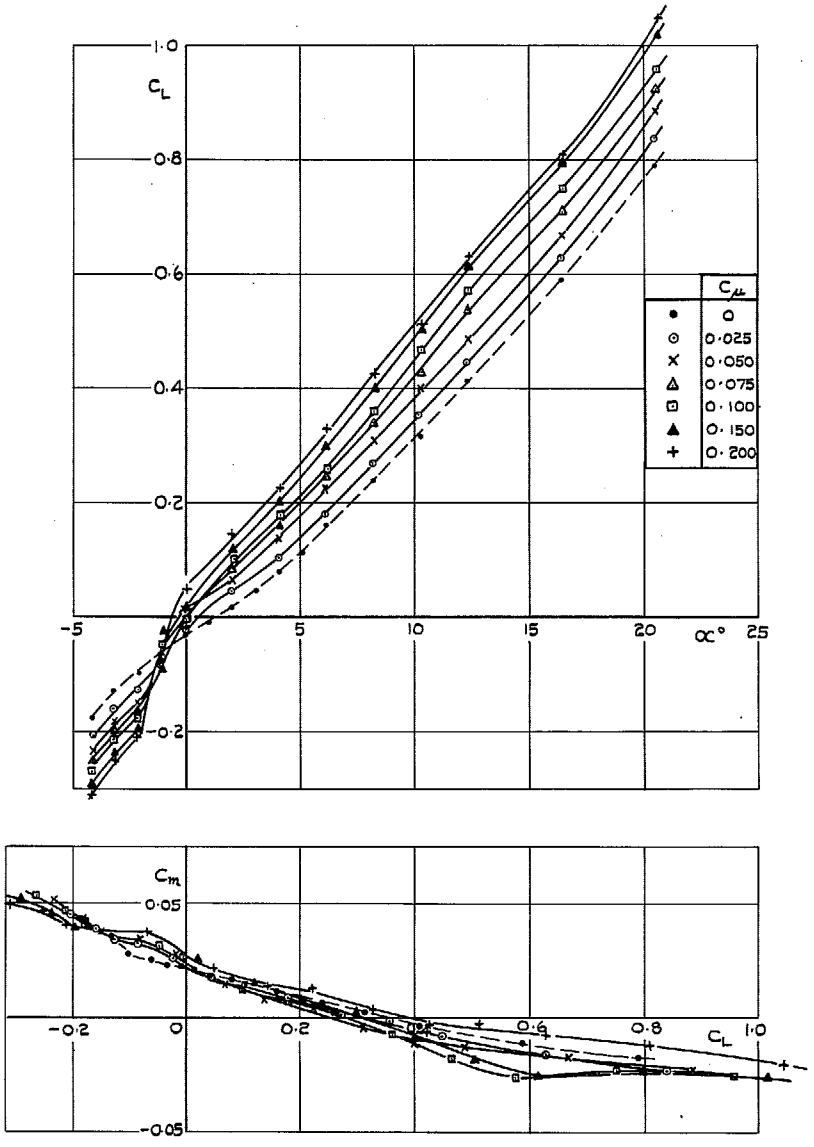

FIG. 7d. Lift and pitching moment. Polygonal slot 'D'.

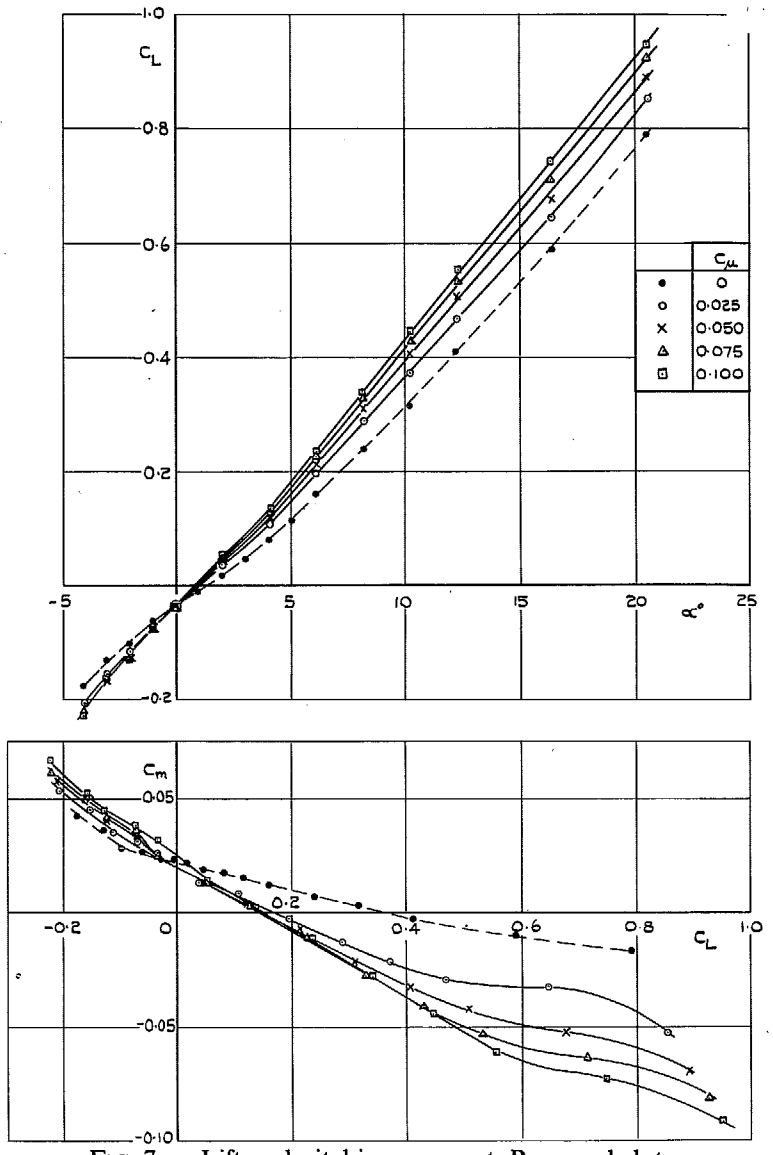

FIG. 7e. Lift and pitching moment. Rear-end slot 'E'.

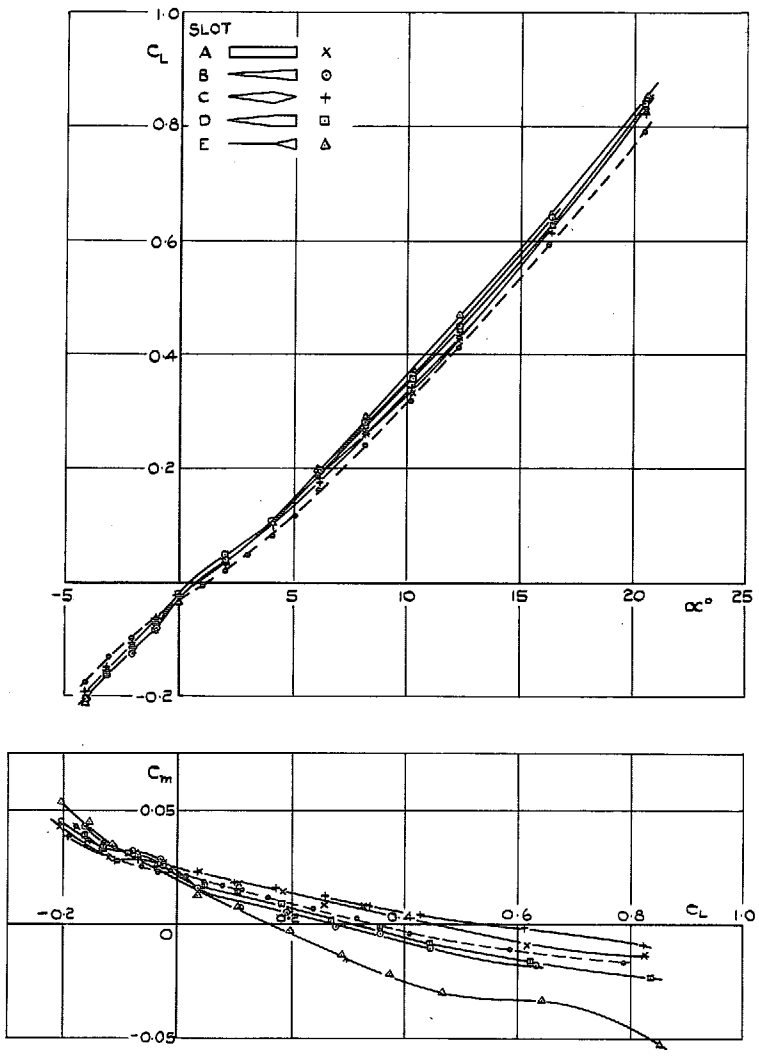

FIG. 8a. Effect of slot shape on lift and pitching moment. ($C_\mu = 0{\cdot}025$).

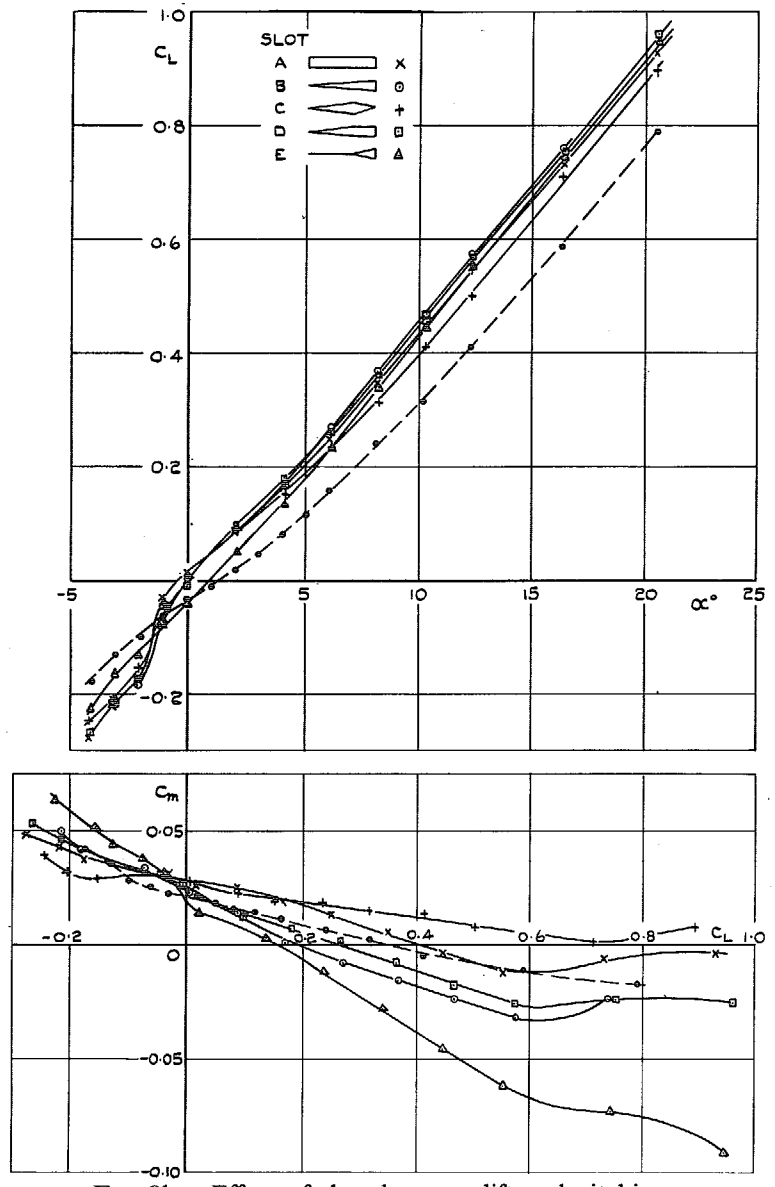

FIG. 8b. Effect of slot shape on lift and pitching moment. ($C_\mu = 0{\cdot}10$).

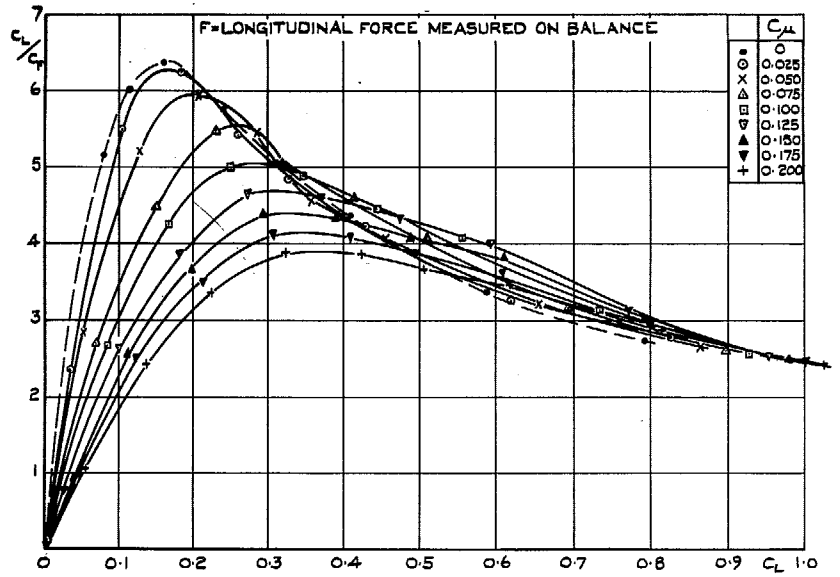

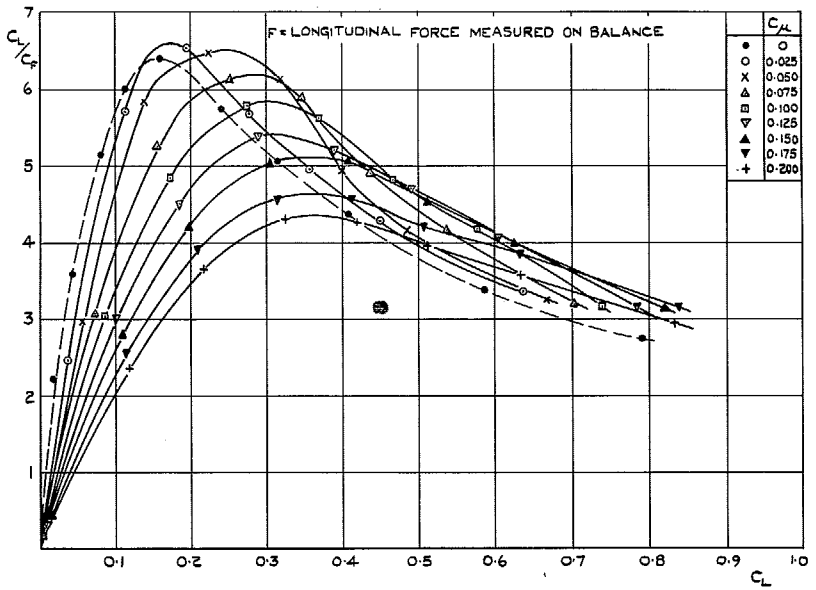

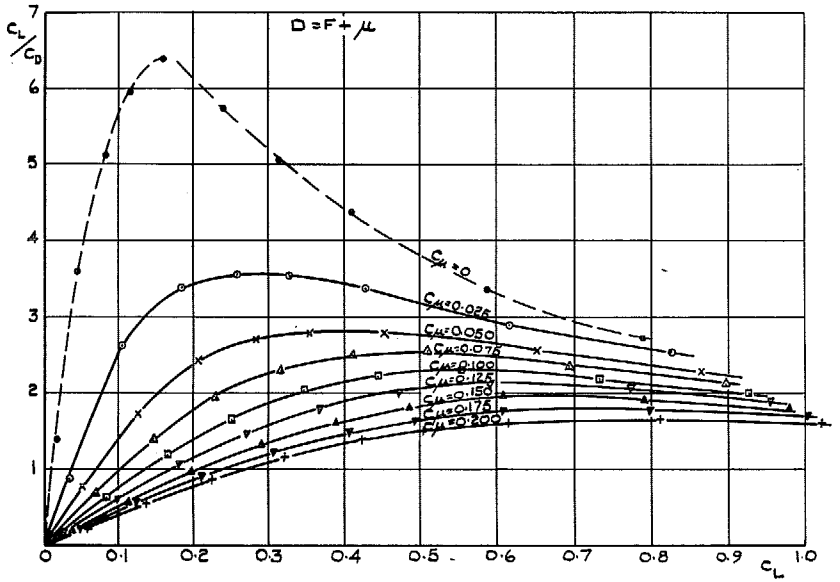

FIG. 9a. Lift/drag ratio. Rectangular slot 'A'.

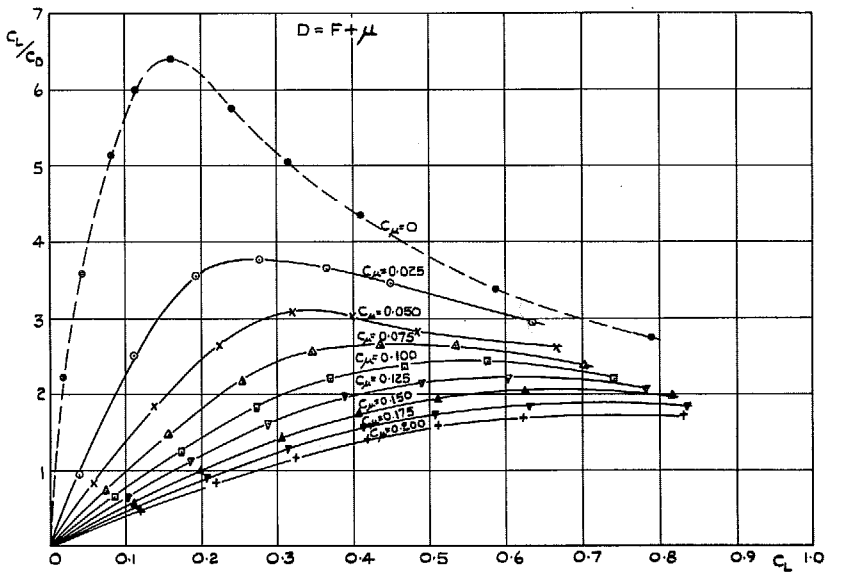

FIG. 9b. Lift/drag ratio. Tapered slot 'B'.

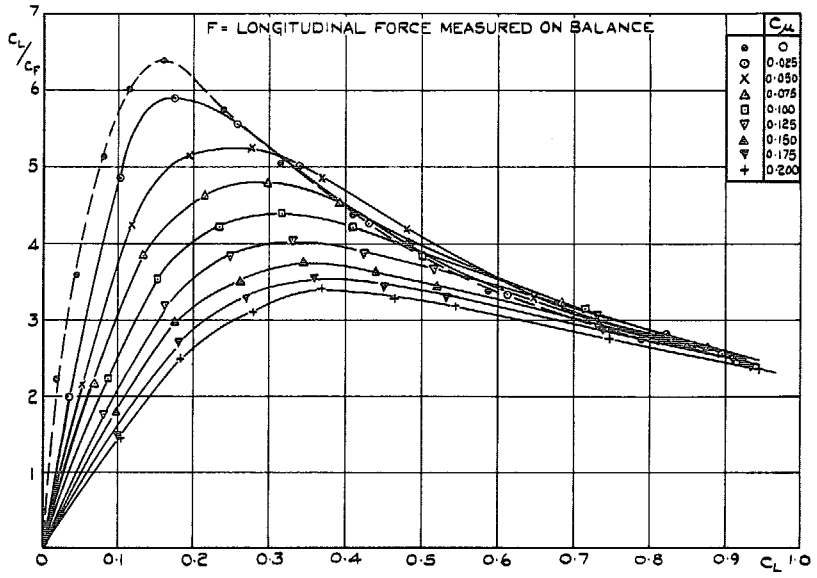

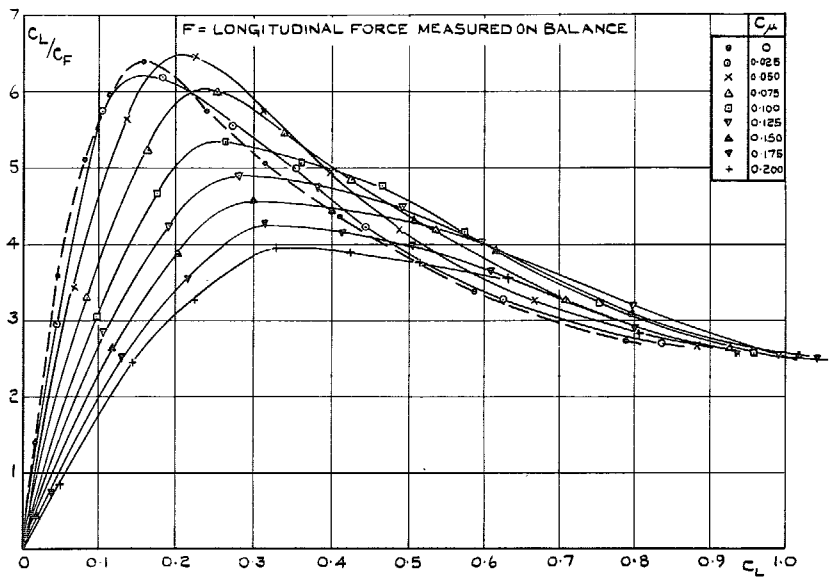

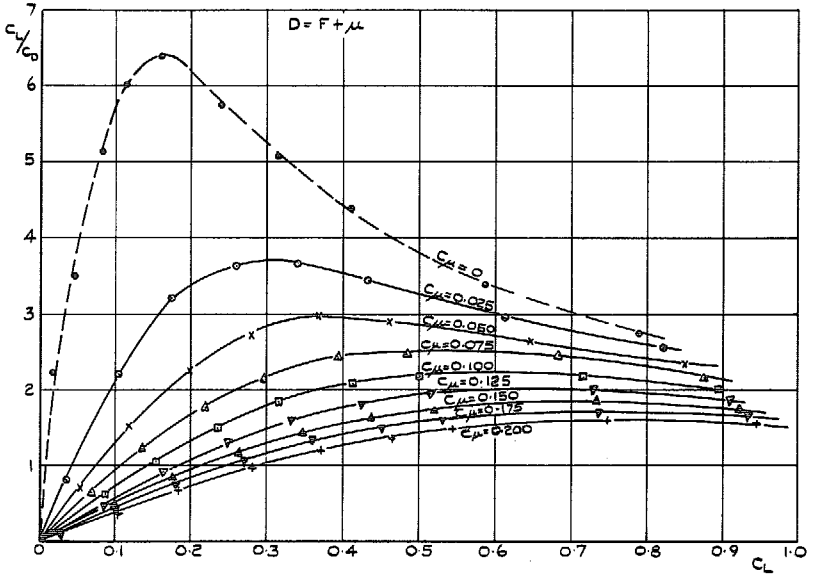

FIG. 9c. Lift/drag ratio. Double tapered slot 'C'.

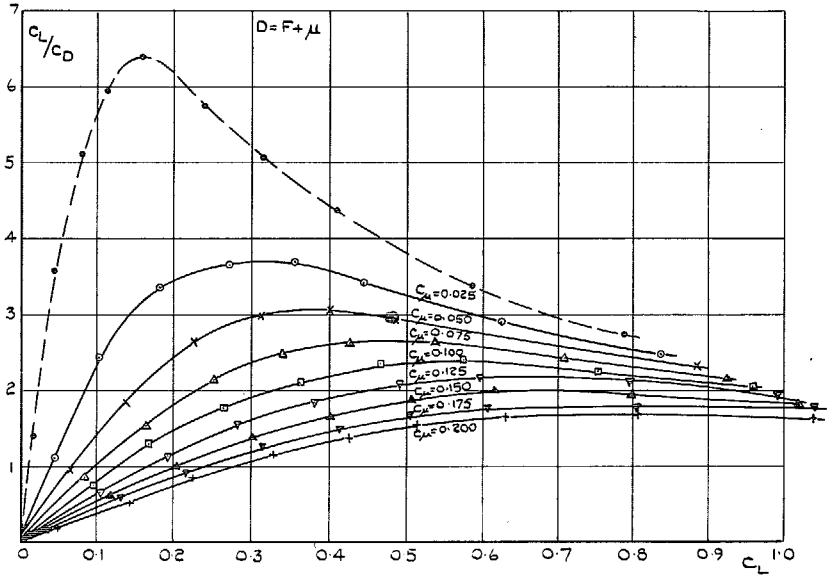

FIG. 9d. Lift/drag ratio. Polygonal slot 'D'.

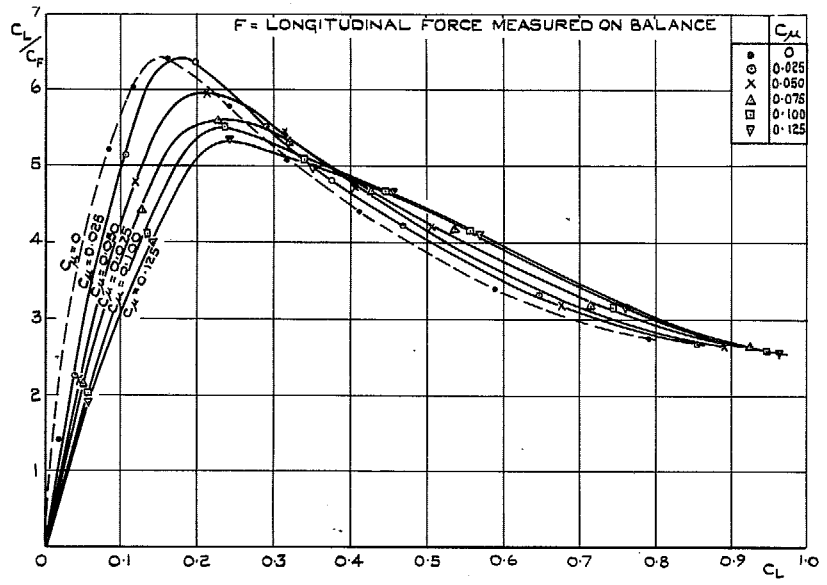

FIG. 9e. Lift/drag ratio. Rear-end slot 'E'.

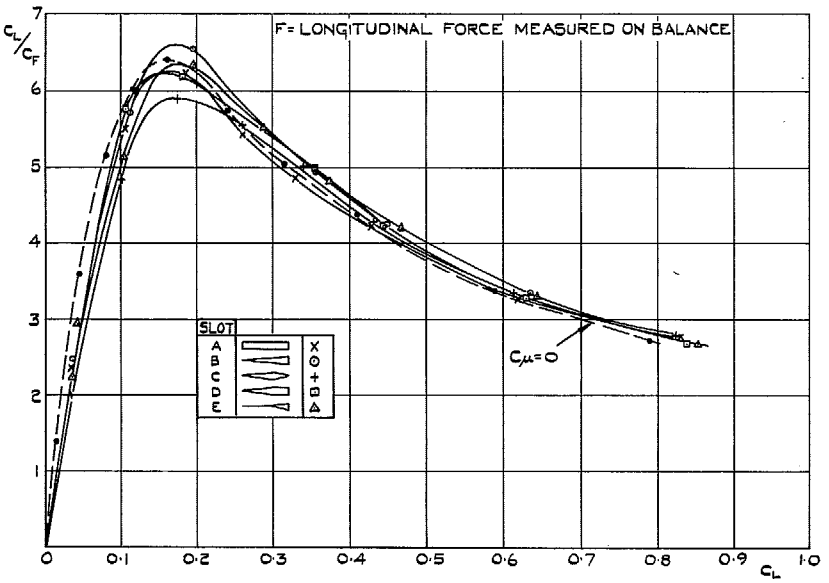

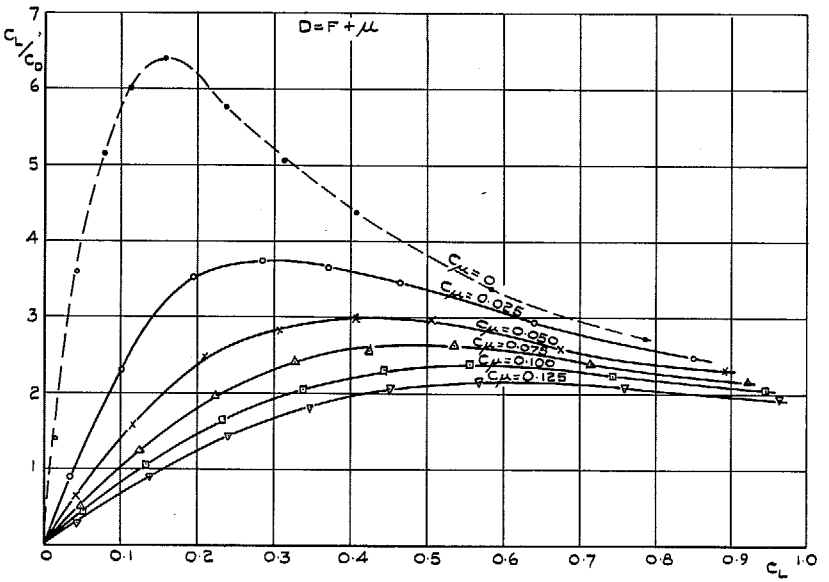

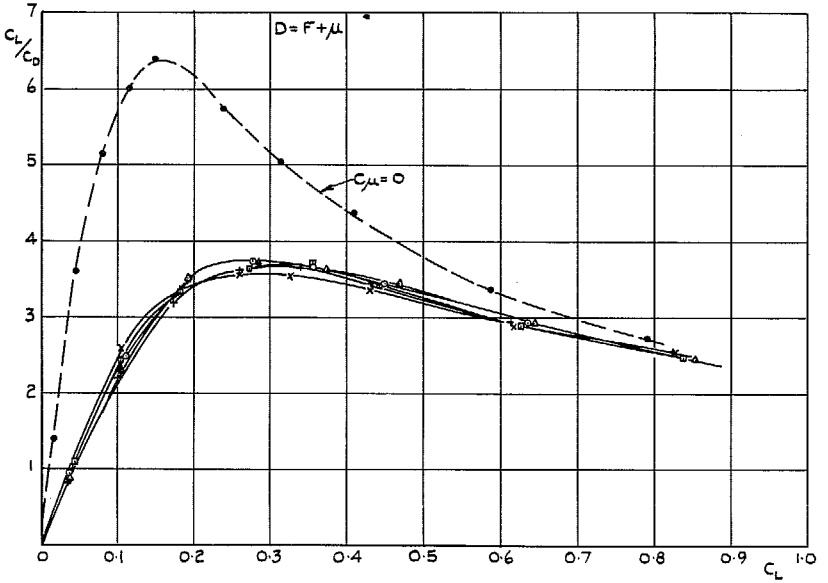

FIG. 10a. Effect of slot shape on lift/drag ratio. ($C\mu = 0{\cdot}025$).

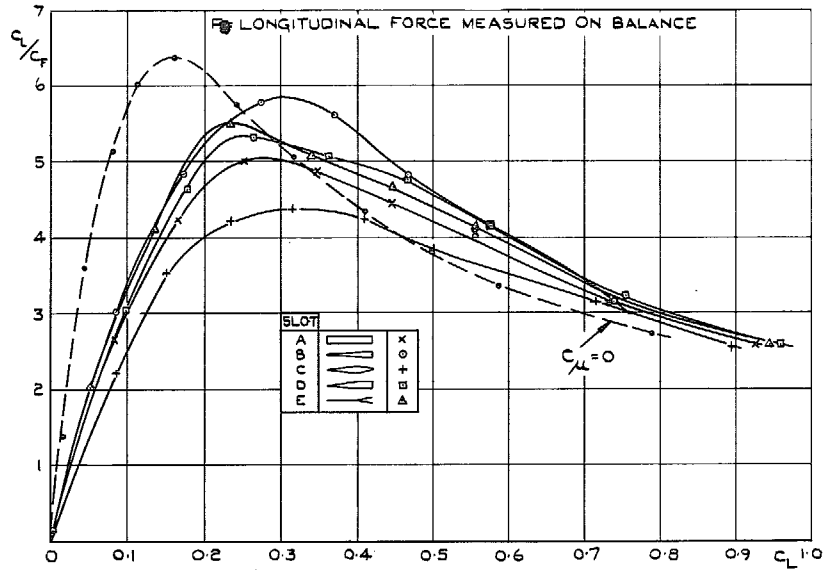

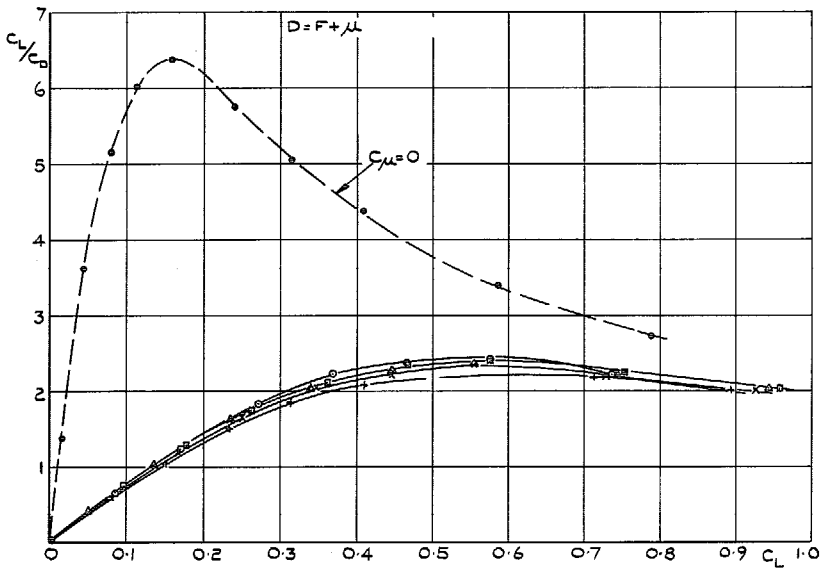

FIG. 10b. Effect of slot shape on lift/drag ratio. ($C\mu = 0{\cdot}10$).

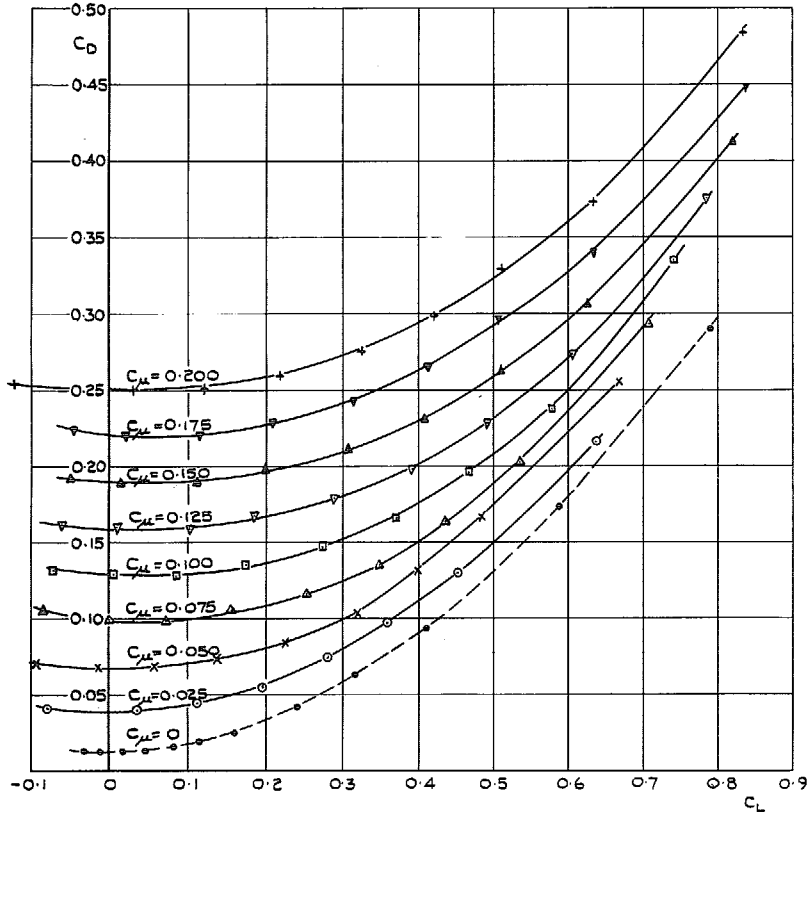

FIG. 11. Drag vs. lift for tapered slot model (slot B).

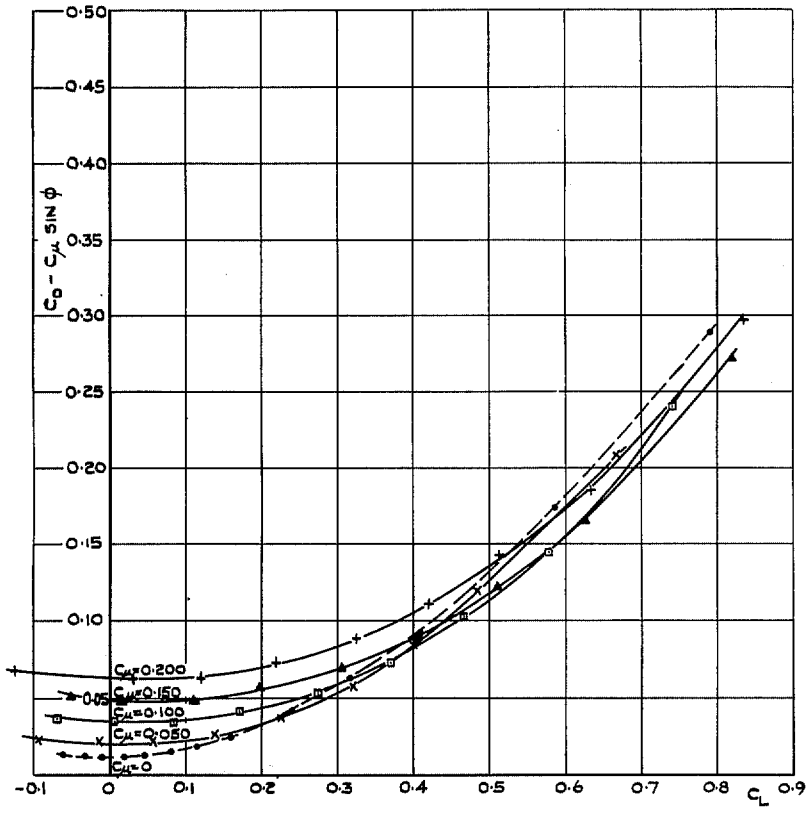

FIG. 12. Drag exclusive of forward component of blowing momentum. Tapered slot 'B'

Printed in Wales for Her Majesty's Stationery Office by Allens Printers (Wales) Limited.

Dd. 129527. K.5.

Published by
HER MAJESTY'S STATIONERY OFFICE

To be purchased from
49 High Holborn, London W.C.1
423 Oxford Street, London W.1
13A Castle Street, Edinburgh 2
109 St. Mary Street, Cardiff CF1 1JW
Brazennose Street, Manchester 2
50 Fairfax Street, Bristol 1
258–259 Broad Street, Birmingham 1
7–11 Linenhall Street, Belfast BT2 8AY
or through any bookseller

S.O. Code No. 23-3518